Journal Pre-proof

Emergence and stability of endoplasmic reticulum network streaming in plant cells

Graham M. Donovan, Congping Lin, Imogen Sparkes, Peter Ashwin

PII: S0022-5193(24)00239-X
DOI: https://doi.org/10.1016/j.jtbi.2024.111954
Reference: YJTBI 111954

To appear in: *Journal of Theoretical Biology*

Received date : 23 May 2024
Revised date : 18 August 2024
Accepted date : 23 September 2024

Please cite this article as: G.M. Donovan, C. Lin, I. Sparkes et al., Emergence and stability of endoplasmic reticulum network streaming in plant cells. *Journal of Theoretical Biology* (2024), doi: https://doi.org/10.1016/j.jtbi.2024.111954.

Highlights

Emergence and stability of endoplasmic reticulum network streaming in plant cells

Graham M Donovan*, Congping Lin*, Imogen Sparkes, Peter Ashwin

- Endoplasmic reticulum (ER) streaming is a key bulk transport process in plant cells.
- This streaming is interrelated with the cytoplasm, ER network and actin-myosin processes.
- We investigate the emergence of ER streaming through interaction of myosin-like motors, actin alignment, and ER network dynamics.

*These authors contributed equally to this work

Emergence and stability of endoplasmic reticulum network streaming in plant cells

Graham M Donovan*[a], Congping Lin*[b], Imogen Sparkes[c], Peter Ashwin[d]

[a]*Department of Mathematics, University of Auckland, Auckland, 1142, New Zealand*
[b]*School of Mathematics and Statistics, Center for Mathematical Sciences & Hubei Key Lab of Engineering Modelling and Scientific, Huazhong University of Science and Technology, Wuhan, China*
[c]*School of Biological Sciences, University of Bristol, Bristol, BS8 1TQ, UK*
[d]*Department of Mathematics and Statistics, University of Exeter, Exeter, EX4 4QF, UK*

Abstract

The endoplasmic reticulum (ER) network is highly complex and highly dynamic in its geometry, and undergoes extensive remodeling and bulk flow. It is known that the ER dynamics are driven by actin-myosin dependent processes. ER motion through the cytoplasm will cause forces on the cytoplasm that will induce flow. However, ER will also clearly be passively transported by the bulk cytoplasmic streaming. We take the complex ER network structure into account and propose a positive-feedback mechanism among myosin-like motors, actin alignment, ER network dynamics for the emergence of ER flow. Using this model, we demonstrate that ER streaming may be an emergent feature of this three-way interaction and that the persistent-point density may be a key driver of the emergence of ER streaming.

Keywords: cytoplasmic streaming, ER streaming, actin, molecular motor

1. Introduction

The endoplasmic reticulum (ER) is an essential organelle in all eukaryotic cells; as well as providing an important reservoir for calcium, it hosts ribosomal activity that translates RNA into proteins and links to the nuclear lumen. In plant cells it can take a variety of forms; it can spread throughout the cytoplasm to form a single interconnected network of tubules and

cisternae that enclose a single lumen ((Kriechbaumer and Brandizzi, 2020) and references therein). Besides persistent regions of the ER network where it is anchored to protein complexes in the plasma membrane (Sparkes et al., 2009a,b; Wang et al., 2014), it is highly complex and highly dynamic in its geometry which undergoes extensive remodeling between persistent areas and bulk flow. It is known that ER dynamics are linked to actin-myosin dependent processes (Sparkes et al., 2009b; Ueda et al., 2010; Griffing et al., 2014; Pain et al., 2023). ER membrane-associated actin-binding proteins (Cao et al., 2016) have been discovered to be important in the striking dynamical rearrangement of the ER over actin.

ER motion through the cytoplasm will cause forces on the cytoplasm that will induce cytoplasmic flow. Meanwhile, ER will also clearly be passively transported by the bulk cytoplasmic streaming. Cytoplasmic streaming has been proposed to play various biological roles including regulation of cell growth and migration, establishment of polarity and cargo delivery (Lu, 2023; Tominaga and Ito, 2015; Shimmen, 2007). This is also powered by molecular motor/cytoskeletal interaction (Kimura et al., 2017). ER streaming has been shown to be correlated with the movement of many other organelles (Stefano et al., 2015).

In investigating the emergence of cytoplasmic streaming, Kimura *et. al.* have proposed a positive-feedback mechanism, where a local flow generated by motors along microtubules is transmitted to neighbouring regions through the ER, and aligns microtubules over a broader area to self-organize the collective flow (Kimura et al., 2017). In plant cells, similarly, Woodhouse *et al.* have considered that myosin motors transmit the forces to the cytoplasm to generate a cell-wide flow, which aligns actin filaments to study the cytoplasmic streaming in *Arabidopsis thaliana* (Woodhouse and Goldstein, 2013). They both modelled the orientation of microtubules or actin filaments by their average polarity and the flow of cytoplasm without considering the complex ER geometric structure.

The ER network geometry, with the development of image processing techniques, can be automatically extracted as a graph representation (Pain et al., 2019; Pain and Kriechbaumer, 2020; Fricker et al., 2024). For instance,in a previous article (Lin et al., 2014), the ER geometry was quantified as a planar graph that connects persistent points, and was considered to be as perturbed Euclidean Steiner networks between persistent points (Lin et al., 2014). The persistent points are potentially the anchor tethering the ER to the plasma membrane. During the network reorganization, the movement of

ER tubular filament has been modelled by balancing surface tension force, Stokes drag force, and Brownian forces (Lin et al., 2017; Lin and Ashwin, 2023).

It is important to note that while movement of the ER may be actively driven through myosins bound to the surface of the ER, it may also be driven indirectly through myosins bound to organelles which are tethered to the ER pulling the ER (Perico and Sparkes, 2018).

The question that motivates this paper is: how do actin alignment and ER dynamics interact with the cytoplasm to produce ER streaming? Does one of these factors drive the others? In this paper we demonstrate in a plausible model that ER streaming may be an emergent feature of the three-way interaction between all three factors (ER dynamics, actin polymerization and cytoplasm flow), rather than one factor driving the others.

2. A model for interaction of actin, cytoplasm and ER

We propose a model where actin organisation, cytoplasmic streaming, ER movement and ER reorganisation interact, and that a feedback loop within those interactions causes the ER streaming to emerge. More precisely, we assume the feedback mechanisms depicted in Fig. 1. That is, we assume that myosin-like motors attached to the ER exert force along the actin cables to exert force which causes ER network motion, and that these forces contribute to ER movement and reorganisation (Lin et al., 2014, 2017; Lin and Ashwin, 2023).

The resulting ER movement is assumed to entrain the cytoplasm. Here, we are considering the myosin-based activity exerted on the ER is either direct on the ER surface or indirectly through movement of organelles attached (i.e. tethered) to the surface of the ER which in turn moves the ER. Note that, while in Nothnagel and Webb (1982) cytoplasmic streaming is modelled as requiring the movement of a large network rather than just spheroid organelles, here we are using the same premise that streaming requires the movement of a large network, namely the ER. Finally, cytoplasm movement contributes to actin cable organisation. The overall idea is similar to Woodhouse and Goldstein (2013) but with the ER network explicitly mediating the interaction between cytoplasm flow and actin cable alignment.

Explicitly the model is as follows. The cytoplasm velocity $\mathbf{u}(x,t)$ is given in units of $\mu m/s$ and governed by 2D stokes flow where

$$\eta\nabla^2\mathbf{u} + \nabla\Pi = \mathbf{F} \tag{1}$$

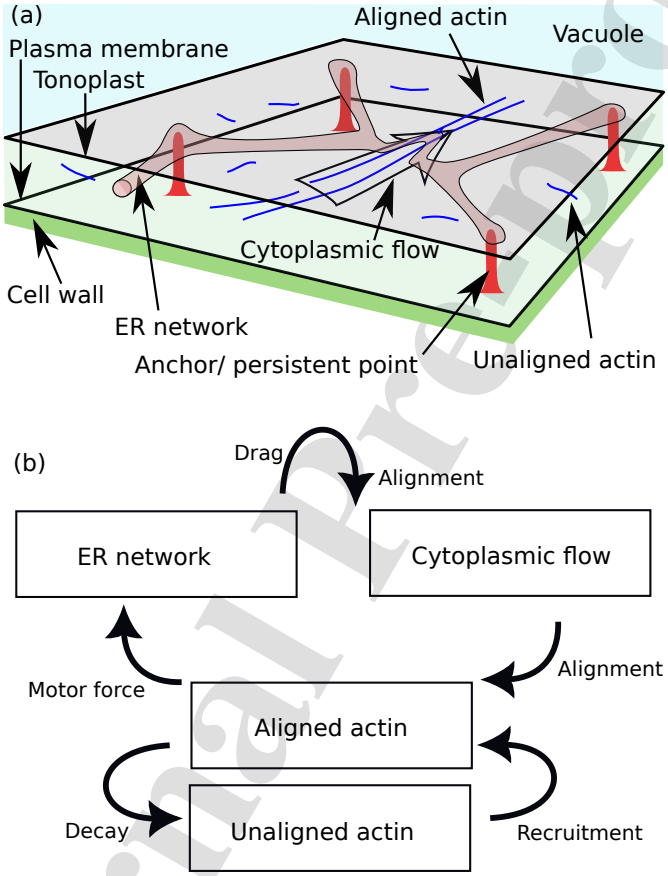

Figure 1: Schematic diagram showing (a) the thin layer of cytoplasm between plasma membrane and vacuole of a plant cell where the ER network resides, and (b) interrelationships between actin filaments and cytoplasmic flow via the ER network. Observe the feedback loop whereby the alignment of acting applies force to move the ER network which, in turn, can induce cytoplasmic flow.

and

$$\nabla \cdot \mathbf{u} = 0. \tag{2}$$

Here Π is the pressure, $\mathbf{F}$ is the fluid forcing due to ER movement and η is the dynamic viscosity. The ER lies within a thin layer of cytoplasm between plasma membrane and vacuole, and here the flow many be reasonably approximated as 2D (Woodhouse and Goldstein, 2013).

For the form of the forcing, we follow Woodhouse and Goldstein (2013) in which two possibilities were considered:

$$\mathbf{F} = \begin{cases} \Phi\dot{\mathbf{x}}, & \text{or} \\ \Phi\dot{\mathbf{x}}|\dot{\mathbf{x}}|^2 \end{cases} \tag{3}$$

Importantly, while Woodhouse and Goldstein (2013) opted for the phenomenological cubic-form nonlinearity for their instability, here with ER intermediation of the actin/flow dynamics we use only simple linear forcing.

We followed the ER network dynamics according to Lin and Ashwin (2023); Lin et al. (2017). Without considering the flow effect, we simulate the network of ER filaments using through cycles of the following steps:

- (a) Meshing filaments into line segments. We mesh straight lines connecting filaments to ensure the each line segment is no larger than $\eta_{\max}$. More specifically, if one segment has length larger than $\eta_{\max}$, then we add a new point at the midpoint and repeat this process until all segments have length no larger than $\eta_{\max}$.

- (b) Movement of filaments according to $\dot{\mathbf{x}} = b\mathbf{\Gamma} + d_1\mathbf{a}$ where $\mathbf{\Gamma} = -\sum_{i=1}^{3} \mathbf{r}_i/|\mathbf{r}_i|$ is the resultant geometric force over directions $\mathbf{r}_i = \mathbf{x}-\mathbf{x}_i$ from the current point x to its 3 neighbors (i.e., nodes directly connected to x) $\mathbf{x}_i$ $(i = 1, 2, 3)$, or $\mathbf{\Gamma} = -\mathbf{K}$ is the signed vector curvature if x is of degree 2. The non-persistent three-way junctions move according to tension and viscous drag.

- (c) We merge two points connected by a line segment if they are no farther than $\eta_{\min}$ apart. We also rearrange connections if there is an intersection between two lines by creating a new point at each intersection and merging with the point closest to the intersection point.

- (d) Splitting nodes if the angle at anchors (of degree 2) is less than $2\pi/3$, or if four or more filaments meet at a junction. More precisely,

we check the angles at the anchors and degree-4 points. If there is an angle of less than $2\pi/3$, then we split the vertex point and create a new point along the bisector of the angle at a distance ϵ. This is repeated until there are no more angles smaller than $2\pi/3$ for degree-2 anchors and degree-4 points.

We remark that four filaments may meet at a junction through the merging process in simulations and splitting process will then be followed. We set $\eta_{\max} = 2\ \mu m$, $\eta_{\min} = 0.01\mu m$ as the minimal segment length, and $\epsilon = 2\eta_{\min}$, following Lin and Ashwin (2023).

Finally we describe the actin dynamics for both unaligned G-actin denoted by the (scalar) α, and aligned F-actin denoted by $\mathbf{f}$, where the vector quantity encodes both the density and direction of alignment. Then we have

$$\dot{\alpha} = \underbrace{k_1}_{\text{production}} - \underbrace{k_2\alpha}_{\text{decay}} + \underbrace{k_3\nabla\alpha}_{\text{diffusion}} - \underbrace{||\sigma(\alpha\mathbf{u} - c_1\mathbf{f})||}_{\text{alignment to F-actin}} \tag{4}$$

and

$$\dot{\mathbf{f}} = \underbrace{\sigma(\alpha\mathbf{u} - c_1\mathbf{f})}_{\text{alignment of G-actin by } \mathbf{u}} - \underbrace{c_2\mathbf{f}}_{\text{decay of F-actin}} \tag{5}$$

with

$$\sigma = \sigma_0\left(1 - \frac{1}{A}\iint_D ||\mathbf{f}||/\bar{f}\ dA\right) \tag{6}$$

enforcing an energetic maximum alignment (where D is the domain and A its area). Aligned F-actin is modelled as a vector quantity so as to encode the average direction of alignment, whereas the (unaligned) G-actin density is a simple scalar. Here we model only the average aligned F-actin direction, rather than defining the angular distribution function overall all directions and then obtaining the average direction and concentration by integration of the distribution (cf. Woodhouse and Goldstein (2013)).

We assume periodic boundary conditions, mimicking a small portion of an infinite (large) domain, given that computational constraints preclude simulation of an entire cell. The spectral numerical method for the flow equations naturally acquires periodic boundary conditions; such conditions are explicitly imposed on the finite difference method for the actin dynamics.

Parameters values are given in Table 1 where the overbar quantities denote equilibrium values. Then a balance calculation suggests $c_1 = \bar{u}\frac{\bar{\alpha}}{|\bar{f}|} - c_2/\sigma_0$. This leaves three free parameters: k_1 (G-actin production), d_1 (ER

Parameter	Estimated range	Assumed value
G-actin diffusivity	3-30 $\mu m^2/s$	$k_3 = 10\ \mu m^2/s$
F-actin dissociation rate	0.27-7.2 s^{-1}	$c_2 = k_2 = 1\ s^{-1}$
total F-actin polymerization rate	0.1-11.6 $\mu M^{-1}s^{-1}$	$\sigma_0 = 0.1\ \mu m^{-1}$
dynamic viscocity	0.7 - 900 cP	$\eta = 0.01\ Pa\ s$
ratio of G:F actin	3.2 $\pm$0.9	$\bar{\alpha}/\|\|\bar{f}\|\| = 3.2$

Table 1: Model parameter values from (Dijksterhuis et al., 2007; Pittman et al., 2022; Kuhn and Pollard, 2005).

network movement by aligned F-actin) and Φ (flow forcing by ER network motion).

The combined model is solved using a spectral fast Poisson solver (Trefethen, 2000) for the Stokes flow, a finite difference scheme for the diffusion of G-actin, and network dynamics as previously described (Lin and Ashwin, 2023). The coupled equations are advanced in time with Euler's method with a timestep of 0.001 s. Two types of initial conditions are used: i) a trivial equilibrium state with zero flow and aligned F-actin, in order to study the emergence of streaming, and ii) a "streaming" initial condition in which a band of aligned F-actin is imposed to mimic an existing stream location.

3. Live cell ER dynamics: imaging data & analysis

We compare features of our models with ER movies taken from spinning-disk confocal imaging of ER in live tobacco epidermal pavement cells. Each movie has a temporal resolution 0.2 s per frame of total 200 frames, and a spatial resolution 0.129 μm per pixel. In a plant cell, the ER lies within a thin layer of cytoplasm between plasma membrane and vacuole, thus, the network of ER can be approximated as a planar graph that connects persistent points which may be embedded within the plasma membrane. In our previous work Lin et al. (2014, 2017) using planar graphs, we have shown that ER tubular network can be understood as the perturbed Euclidean Steiner network between persistent points. Persistent points are extracted using the similar approach as in (Lin et al., 2014) by local maximum of the averages of pixel intensities over the entire movie. More precisely, an average image with pixel intensities averaged over the entire movie is created, and masked by a threshold and then local maximum is extracted as the persistent points. Here the threshold is 0.45 multiplied by the maximum of the averaged inten-

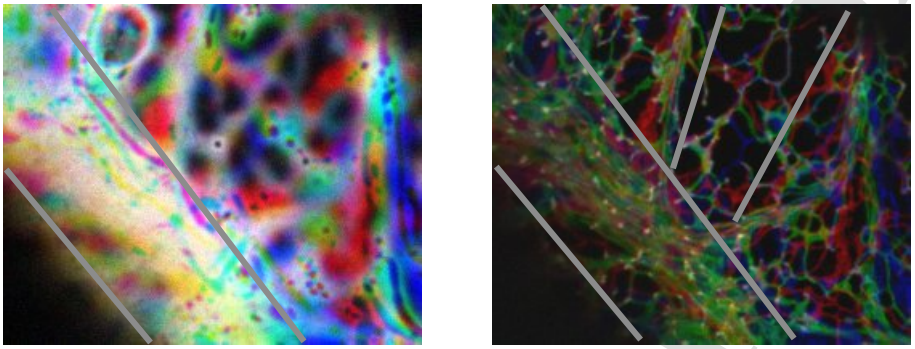

Figure 2: An example of experimental cytoplasmic (left) and ER (right) dynamics. Three frames coloured in red, green and blue with a 10 s time gap between each, are overlaid; gray lines highlight cytoplasmic streaming part (left), ER streaming and ER network reorganisation without streaming (right), during the observed time period. The white spots (areas) in ER (right panel) are persistent spots.

sity among all pixels for two movies respectively. The threshold is manually chosen to be robust for the extraction of persistent points.

In different regions of the same movie, the threshold for identifying persistent points are the same. Also note that in actual ER movies, the ER streaming region is transient. To compare the persistent points within streaming and away from streaming, we particularly choose regions that the ER streaming occurs or does not occur over the entire movie. In particular, we choose regions of size 4.5×4.5 μm^2 for analysis. Fig. 2 illustrates an example of movement of cytoplasm and ER network from live imaging where streaming occurs.

4. Results

4.1. Stream persistence and emergence

Streaming is persistent in the model, as demonstrated in Fig. 3. Here we have used an initial condition to establish the streaming, in which the F-actin field is aligned in an initial vertical strip in order to initiate streaming. The streams appear to persist over the simulation period(s), although long simulations are precluded by the computational cost of simulating during ER flow, in which many network dynamics events must be resolved.

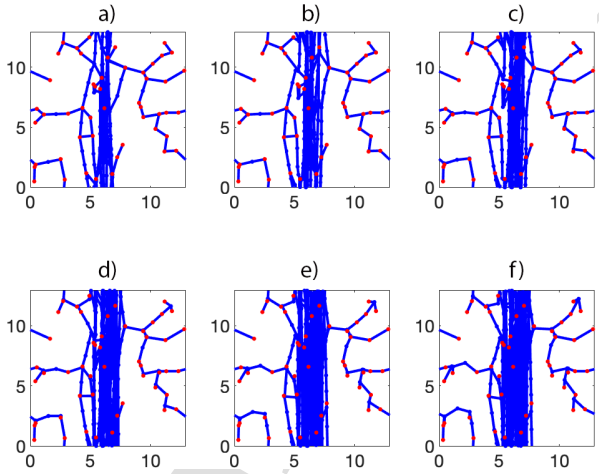

Figure 3: Persistence of ER streaming from an initial streaming configuration. Time snapshots are evenly spaced and increasing in time (0.5s intervals) from panel a) through f). Parameter values as given in the text (Sec 2). Spatial domain in μm. Red: persistent points; blue: ER network. Here $k_1 = 5$, $d_1 = 50$ and $\Phi = 0.01$.

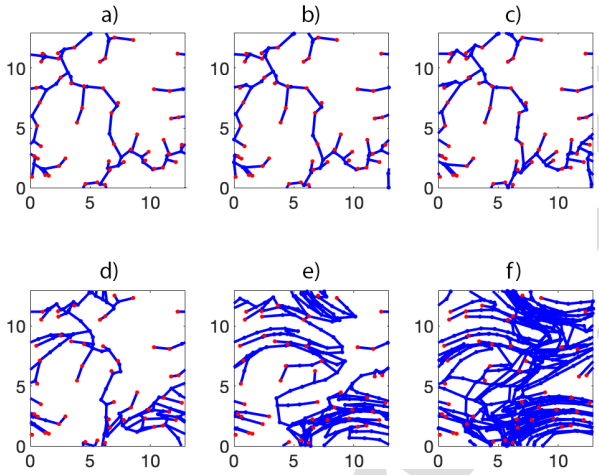

Figure 4: Emergence of ER streaming from an initial zero-velocity configuration. Time snapshots are evenly spaced and increasing in time (0.5s intervals) from panel a) through f). Here the parameter values of k_1, d_1 and Φ have all been increased by $\sqrt[3]{10}$ compared with the simulation in Fig. 3.

Streaming persistence is a minimal and expected behaviour. More interesting is the potential for streaming to emerge from a trivial initial state. One such example in simulation is shown in Fig. 4. The direction of streaming here is a consequence of the (stochastic) persistent point placement and initial network configuration. Contra-flow necessarily emerges due to the periodic boundary conditions.

The stream velocity and actin dynamics for these example simulations are shown in Fig. 5. Note the log scale for the stream velocity. Thus we can see the existence of streaming and non-streaming states in the same part of parameter space, and also of emergence (with altered parameters). This of course is only a single example in simulation, but it demonstrates the potential. In the next section we examine the stability boundaries for the emergence of streaming.

4.2. Emergence stability analysis

In order to investigate emergence of streaming we linearise about the trivial state as

$$(\mathbf{u}, \mathbf{f}, \alpha) = (0, 0, k_1/k_2) + \epsilon(\hat{u}\mathbf{e}_1, \hat{f}\mathbf{e}_1, \hat{\alpha}) \tag{7}$$

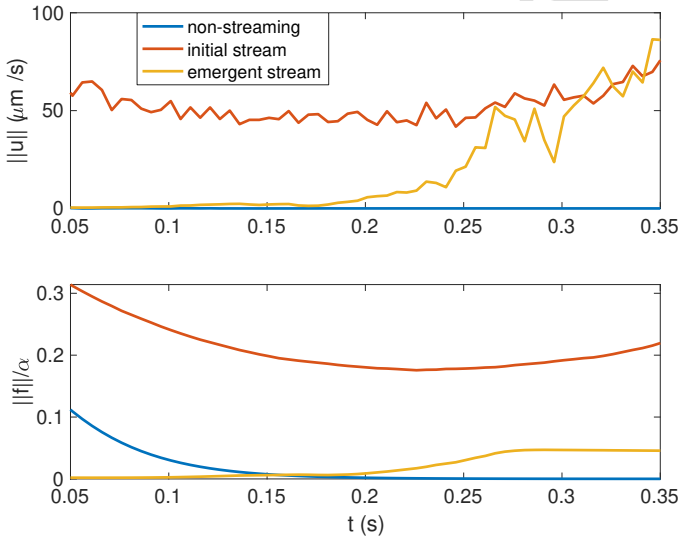

Figure 5: Comparison of the stream velocity and actin dynamics of the emergence and streaming configurations in Figs. 3 and 4. Upper panel: stream speed at the center of the domain ($\mu m/s$); lower panel: ratio of aligned F-actin to G-actin $||\mathbf{f}||/\alpha$ at the same point. The streaming and non-streaming conditions use the same parameter values, but different initial conditions (established stream vs. uniform actin field). The emergence case has altered parameters as described in the Fig. 4 caption.

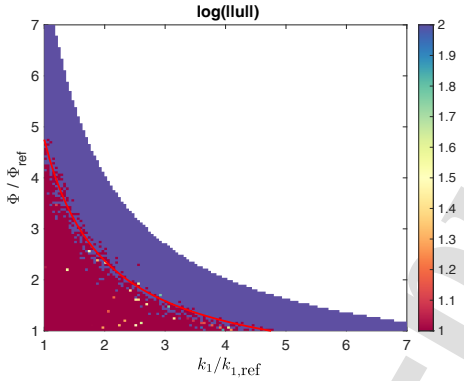

Figure 6: Testing the stability boundary: emergence of streaming from simulations (background colormap) compared with predictions from linear stability analysis (Eq. 10, red line overlaid).

using an arbitrary unit direction $\mathbf{e}_1$. This yields, at leading order

$$\dot{\hat{f}} = \sigma_0 \left(\frac{k_1}{k_2} \hat{u} - c_1 \hat{f} \right) - c_2 \hat{f} \tag{8}$$

which is independent of $\hat{\alpha}$. Assuming that the cytoplasm velocity response is dependent on aligned F-actin (via ER movement) as

$$\eta \hat{u} = \Phi d_1 h(\hat{f}) \tag{9}$$

for some h (where $h(0) = 0$ and $h' > 0$), stability requires

$$\sigma_0 \frac{k_1}{k_2} \frac{\Phi d_1}{\eta} h'(0) > \sigma_0 c_1 + c_2. \tag{10}$$

Of course we do not know the form of h, but nonetheless the parametric dependence here is informative: we can infer the value of $h'(0)$ from simulation data and explore the accuracy of the predicted stability boundary in the free parameter space. This estimate is compared with emergence from simulations in Fig. 6; up to a constant of proportionality (because of the unknown form of h and thus the value of $h'(0)$), the functional dependence of the instability on k_1, d_1 and Φ appears to be very accurate.

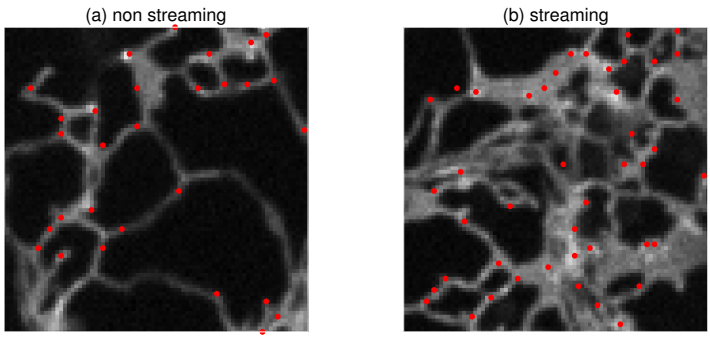

Figure 7: Example of ER persistent points in non-streaming (left) and streaming region (b) during one movie observation. Red points indicate the extracted persistent points.

4.3. Emergence/streaming behaviour and persistent point density

In the above analysis we have not explicitly taken into account the spatial structure of the ER network. One intriguing hypothesis is that the emergence and/or persistence of streaming might depend on the local structure of the network; the most convenient proxy for network structure is the persistent point density. An example from experimental movies, comparing streaming and non-streaming frames, is shown in Fig. 7.

In order to test the hypothesis that streaming is related to persistent point density, we compared persistent point counts in streaming and non-streaming frames, as shown in Fig. 8 for two different movies. The difference in persistent point density between streaming and non-streaming regions is statistically significant for movie 2, but not for movie 1, suggesting plausible support for the underlying hypothesis. For purposes of comparison, we performed Monte Carlo simulations of the model with randomised persistent point locations, and identified the locus of streaming emergence for 100 simulations; the persistent point density at these locations is compared with the (prescribed) average persistent point density in the entire simulation domain. Across both movies and simulations, there is a strongly significant relationship between streaming and persistent point density as shown in Fig. 8 (statistical tests described in figure caption). Taken together these results suggest that persistent point density may be an important determinant of stream emergence and location.

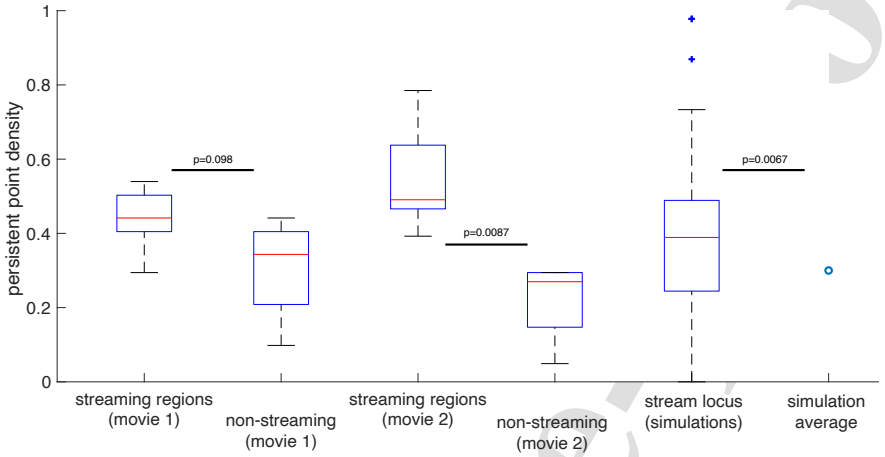

Figure 8: Streaming/non-streaming density comparisons. Movie streaming region point counts as described in Sec. 3, comparison by two-sample t-test. Simulation streaming locus comparison by one-sample t-test (relative to prescribed simulation average density).

5. Discussion & Conclusions

Cytoplasmic streaming in plant cells is an intriguing transport phenomenon, and although its emergence via instability has been studied previously, there is not a clear consensus on what causes it. In this paper we investigate a model that incorporates ER network dynamics into the streaming process. In our model, the ER network dynamics are an important contributor but the streaming only appear because of the three-way interaction between ER dynamics, actin and cytoplasmic flow. In support of this, there appears to be a significant relationship between persistent point density and streaming, in the experimental movies and this is reflected in the model simulations. Specifically, there is a higher persistent point density in streaming regions compared with non-streaming regions (movies) and at stream emergence locations compared with average density (simulations). At the very least, this supports the idea that ER network modulation is an important part of the streaming process.

In reality, the interactions will be more complex than shown in Fig. 1 – for example, the cytoplasmic flow will advect the ER networks as well as being dragged by it. Indeed, we observe that there are more realistic (and more computationally intensive) models of ER/flow interaction Lin and Ash-

win (2023) where the interaction can occurs along the length of the filaments. However, our aim here is to produce a minimal model where streaming can emerge rather than to include all biophysical effects. One important point is that while Woodhouse and Goldstein (2013) opted for a phenomenological cubic form nonlinearity in order to generate the instability leading to emergence of streaming, here with introduction of ER mediation of the actin/flow relationship we are able to use a simple linear relationship. We have also simplified by considering only the average aligned F-actin direction, rather than defining the angular distribution function for all directions and then obtaining the average direction and concentration by averaging over all directions (cf. Woodhouse and Goldstein (2013)).

The comparison between model and experiment is clearly hindered by the limitations of each. Strictly speaking, only some of the phenomena in the model can currently be observed in the experiments. In the experiments, we have access to persistence of streaming (i.e. established streaming and non-streaming regions), but not to stream emergence itself. Experimental capture of stream emergence would require observation of regions that are not streaming and then begin to stream. This could potentially be artificially induced through depolymerisation of actin and observing how streaming emerges as actin begins to polymerise again. However, the experimental limitation is further compounded by technical limitations; this would require a fast imaging system to capture sequential images of an entire cell volume and waiting for streaming to re-emerge. On the simulation side, access to emergence locations is straightforward, but assessing persistence is challenging because of computational costs.

Computational cost limits the simulations in several ways. One is that once streaming emerges, the number of network events that must be resolved increases substantially, which in practice increases hugely the ratio of wall time (elapsed real time) to simulation time for streaming as compared to non-streaming. Similarly, computational cost restricts the practical domain size. For these relatively small domains (i.e. much smaller than a whole cell), periodic boundary conditions are the most appropriate choice, but this means that streaming, once underway, occurs throughout the domain. As such, in practice, on the experimental side we can assess persistence but not emergence, and on the simulation side we can study emergence but not persistence. One potential avenue of remedy is stability analysis of the streaming state (as opposed to the non-streaming state as undertaken in Sec. 4.2), which remains an area for future work. Nonetheless, the relationship between streaming and

persistent point density, in both model and experiment, suggest that ER network dynamics play an important role in modulating streaming.

Acknowledgement

C.L. acknowledges financial support from National Natural Science Foundation of China (NSFC, Grant No. 12171179). P.A. thanks EPSRC for partial support via EPSRC grant EP/T017856/1.

References

Cao, P., Renna, L., Stefano, G., Brandizzi, F., 2016. Syp73 anchors the ER to the actin cytoskeleton for maintenance of ER integrity and streaming in arabidopsis. Current biology 26, 3245–3254.

Dijksterhuis, J., Nijsse, J., Hoekstra, F., Golovina, E., 2007. High viscosity and anisotropy characterize the cytoplasm of fungal dormant stress-resistant spores. Eukaryotic cell 6, 157–170.

Fricker, M., Breeze, E., Pain, C., Kriechbaumer, V., Aguilar, C., Ugalde, J.M., Meyer, A.J., 2024. Quantitation of er morphology and dynamics. Methods in Molecular Biology 2772, 49–75.

Griffing, L.R., Gao, H.T., Sparkes, I., 2014. ER network dynamics are differentially controlled by myosins xi-k, xi-c, xi-e, xi-i, xi-1, and xi-2. Frontiers in plant science 5, 218.

Kimura, K., Mamane, A., Sasaki, T., Sato, K., Takagi, J., Niwayama, R., Hufnagel, L., Shimamoto, Y., Joanny, J.F., Uchida, S., Kimura, A., 2017. Endoplasmic-reticulum-mediated microtubule alignment governs cytoplasmic streaming. Nature Cell Biology 19, 399–406.

Kriechbaumer, V., Brandizzi, F., 2020. The plant endoplasmic reticulum: an organized chaos of tubules and sheets with multiple functions. Journal of Microscopy 280, 122–133.

Kuhn, J.R., Pollard, T.D., 2005. Real-time measurements of actin filament polymerization by total internal reflection fluorescence microscopy. Biophysical Journal 88, 1387–1402.

Lin, C., Ashwin, P., 2023. Geometric dynamics of anchored filamentous networks subject to viscous flow. Communications in Nonlinear Science and Numerical Simulation 118, 107012.

Lin, C., White, R.R., Sparkes, I., Ashwin, P., 2017. Modeling endoplasmic reticulum network maintenance in a plant cell. Biophysical journal 113, 214–222.

Lin, C., Zhang, Y., Sparkes, I., Ashwin, P., 2014. Structure and dynamics of ER: minimal networks and biophysical constraints. Biophysical journal 107, 763–772.

Lu, Wen Gelfand, V.I., 2023. Go with the flow – bulk transport by molecular motors. Journal of Cell Science 136, jcs260300.

Nothnagel, E.A., Webb, W., 1982. Hydrodynamic models of viscous coupling between motile myosin and endoplasm in characean algae. The Journal of cell biology 94, 444–454.

Pain, C., Kriechbaumer, V., 2020. Defining the dance: quantification and classification of endoplasmic reticulum dynamics. Journal of Experimental Botany 71, 1757–1762.

Pain, C., Kriechbaumer, V., Kittelmann, M., Hawes, C., Fricker, M., 2019. Quantitative analysis of plant er architecture and dynamics. Nature Communications 10, 984.

Pain, C., Tolmie, F., Wojcik, S., Wang, P., Kriechbaumer, V., 2023. interacting: The structure and dynamics of er and actin are interlinked. Journal of Microscopy 291, 105–118.

Perico, C., Sparkes, I., 2018. Plant organelle dynamics: cytoskeletal controland membrane contact sites. New Phytologist , 381–394.

Pittman, M., Iu, E., Li, K., Chen, J., Potnikov, S., Chen, Y., 2022. Membrane ruffling is a mechanosensor of extracellular fluid viscosity. Biophysical Journal 121, 267a.

Shimmen, T., 2007. The sliding theory of cytoplasmic streaming: fifty years of progress. Journal of plant research 120, 31–43.

Sparkes, I., Ketelaar, T., de Ruijter, N.C.A., Hawes, C., 2009a. Grab a Golgi: laser trapping of Golgi bodies reveals in vivo interactions with the endoplasmic reticulum. Traffic 10, 567–571.

Sparkes, I., Runions, J., Hawes, C., Griffing, L., 2009b. Movement and remodeling of the endoplasmic reticulum in nondividing cells of tobacco leaves. The Plant Cell 21, 3937–3949.

Stefano, G., Renna, L., Lai, Y., Slabaugh, E., Mannino, N., Buono, R.A., Otegui, M.S., Brandizzi, F., 2015. ER network homeostasis is critical for plant endosome streaming and endocytosis. Cell Discovery 1, 15033.

Tominaga, M., Ito, K., 2015. The molecular mechanism and physiological role of cytoplasmic streaming. Current Opinion in Plant Biology 27, 104–110.

Trefethen, L.N., 2000. Spectral methods in MATLAB. SIAM.

Ueda, H., Yokota, E., Kutsuna, N., Shimada, T., Tamura, K., Shimmen, T., Hasezawa, S., Dolja, V.V., Hara-Nishimura, I., 2010. Myosin-dependent endoplasmic reticulum motility and f-actin organization in plant cells. Proceedings of the National Academy of Sciences 107, 6894–6899.

Wang, P., Hawkins, T.J., Richardson, C., Cummins, I., Deeks, M.J., Sparkes, I., Hawes, C., Hussey, P.J., 2014. Report the plant cytoskeleton , net3c , and vap27 mediate the link between the plasma membrane and endoplasmic reticulum. Current Biology 24, 1397–1405.

Woodhouse, F.G., Goldstein, R.E., 2013. Cytoplasmic streaming in plant cells emerges naturally by microfilament self-organization. Proceedings of the National Academy of Sciences 110, 14132–14137.

No conflicts of interest to declare.